

Dynamic Balancing of Isoprene Carbon Sources Reflects Photosynthetic and Photorespiratory Responses to Temperature Stress¹[W][OPEN]

Kolby Jardine*, Jeffrey Chambers, Eliane G. Alves, Andrea Teixeira, Sabrina Garcia, Jennifer Holm, Niro Higuchi, Antonio Manzi, Leif Abrell, Jose D. Fuentes, Lars K. Nielsen, Margaret S. Torn, and Claudia E. Vickers

Climate Science Department, Earth Science Division, Lawrence Berkeley National Laboratory, Berkeley, California 94720 (K.J., J.C., J.H., M.S.T.); National Institute for Amazon Research, Manaus, Amazonas 69080–971, Brazil (E.G.A., A.T., S.G., N.H., A.M.); Departments of Chemistry and Biochemistry and Soil, Water, and Environmental Science, University of Arizona, Tucson, Arizona 85721 (L.A.); Department of Meteorology, College of Earth and Mineral Sciences, Pennsylvania State University, University Park, Pennsylvania 16802 (J.D.F.); and Australian Institute for Bioengineering and Nanotechnology, The University of Queensland, Brisbane, St. Lucia, Queensland 4072, Australia (L.K.N., C.E.V.)

ORCID ID: 0000-0001-8491-9310 (K.J.).

The volatile gas isoprene is emitted in teragrams per annum quantities from the terrestrial biosphere and exerts a large effect on atmospheric chemistry. Isoprene is made primarily from recently fixed photosynthate; however, alternate carbon sources play an important role, particularly when photosynthate is limiting. We examined the relative contribution of these alternate carbon sources under changes in light and temperature, the two environmental conditions that have the strongest influence over isoprene emission. Using a novel real-time analytical approach that allowed us to examine dynamic changes in carbon sources, we observed that relative contributions do not change as a function of light intensity. We found that the classical uncoupling of isoprene emission from net photosynthesis at elevated leaf temperatures is associated with an increased contribution of alternate carbon. We also observed a rapid compensatory response where alternate carbon sources compensated for transient decreases in recently fixed carbon during thermal ramping, thereby maintaining overall increases in isoprene production rates at high temperatures. Photorespiration is known to contribute to the decline in net photosynthesis at high leaf temperatures. A reduction in the temperature at which the contribution of alternate carbon sources increased was observed under photorespiratory conditions, while photosynthetic conditions increased this temperature. Feeding [2-¹³C]glycine (a photorespiratory intermediate) stimulated emissions of [¹³C_{1–5}]isoprene and ¹³CO₂, supporting the possibility that photorespiration can provide an alternate source of carbon for isoprene synthesis. Our observations have important implications for establishing improved mechanistic predictions of isoprene emissions and primary carbon metabolism, particularly under the predicted increases in future global temperatures.

Many plant species emit isoprene (2-methyl-1,3-butadiene [C₅H₈]) into the atmosphere at high rates (Sharkey and Yeh, 2001). With an estimated emission rate of 500 to 750 teragram per year by terrestrial ecosystems (Guenther et al., 2006), isoprene exerts a strong control over the oxidizing capacity of the atmosphere. Due to its high reactivity to oxidants, it fuels an array of atmospheric chemical and physical processes affecting air quality and climate, including the production of ground-level

ozone in environments with elevated concentrations of nitrogen oxides (Atkinson and Arey, 2003; Pacifico et al., 2009) and the formation/growth of organic aerosols (Nguyen et al., 2011). At the plant level, isoprene provides protection from stress, through stabilizing membrane processes (Sharkey and Singsaas, 1995; Velikova et al., 2011) and/or reducing the accumulation of damaging reactive oxygen species in plant tissues under stress (Loreto et al., 2001; Vickers et al., 2009b; Velikova et al., 2012). While the mechanism(s) are still under investigation, isoprene may directly or indirectly stabilize hydrophobic interactions in membranes (Singsaas et al., 1997), minimize lipid peroxidation (Loreto and Velikova, 2001), and directly react with reactive oxygen species (Kameel et al., 2014), yielding first-order oxidation products methyl vinyl ketone and methacrolein (Jardine et al., 2012, 2013). The two main environmental drivers for global changes in isoprene fluxes are light and temperature (Guenther et al., 2006). Isoprene production is closely linked to net photosynthesis, and both isoprene emissions and net photosynthesis are controlled by light intensity (Monson and Fall, 1989). There is also a positive

¹ This work was supported by the Office of Biological and Environmental Research of the U.S. Department of Energy (under contract no. DE-AC02-05CH11231) as part of their Terrestrial Ecosystem Science Program and the National Science Foundation CHE0216226.

* Address correspondence to kjardine@lbl.gov.

The author responsible for distribution of materials integral to the findings presented in this article in accordance with the policy described in the Instructions for Authors (www.plantphysiol.org) is: Kolby Jardine (kjardine@lbl.gov).

^[W] The online version of this article contains Web-only data.

^[OPEN] Articles can be viewed online without a subscription.

www.plantphysiol.org/cgi/doi/10.1104/pp.114.247494

correlation between net photosynthesis and isoprene emissions as leaf temperatures increase up to the optimum temperature for net photosynthesis (Monson et al., 1992).

Despite the close correlation between photosynthesis and isoprene emissions, plant enclosure observations and leaf-level analyses have both shown that the fraction of net photosynthesis dedicated to isoprene emissions is not constant. During stress events that decrease net photosynthetic rates, isoprene emissions are often less affected or even stimulated; this results in an increase in relative isoprene production from 1% to 2% of net photosynthesis under normal conditions to 15% to 50% under extreme stress (Goldstein et al., 1998; Fuentes et al., 1999; Kesselmeier et al., 2002; Harley et al., 2004). In severe stress conditions such as drought, isoprene emissions can even continue in the complete absence of photosynthesis (Fortunati et al., 2008). An uncoupling of isoprene emissions from net photosynthesis has also been observed in a number of other studies where the optimum temperature for isoprene emissions was found to be substantially higher than that of net photosynthesis; under the high-temperature conditions, isoprene emissions can account for more than 50% of net photosynthesis (Sharkey and Loreto, 1993; Lerdau and Keller, 1997; Harley et al., 2004; Magel et al., 2006).

Analyses of carbon sources using $^{13}\text{CO}_2$ leaf labeling have revealed that under standard conditions (i.e. leaf temperature of 30°C and photosynthetically active radiation [PAR] levels of 1,000 $\mu\text{mol m}^{-2} \text{s}^{-1}$), isoprene is produced primarily (70%–90%) using carbon directly derived from the Calvin cycle (Delwiche and Sharkey, 1993; Affek and Yakir, 2002; Karl et al., 2002) via the chloroplastic methylerythritol phosphate (MEP) isoprenoid pathway (Zeidler et al., 1997). The relative contributions of photosynthetic and alternate carbon sources for isoprene are now recognized as being variable under different environmental conditions. Changes in net photosynthesis rates under drought stress (Funk et al., 2004; Brilli et al., 2007), salt stress (Loreto and Delfine, 2000), and changes in ambient O_2 and CO_2 concentrations (Jones and Rasmussen, 1975; Karl et al., 2002; Trowbridge et al., 2012) alter their relative contributions. Under heat stress-induced photosynthetic limitation in *Populus deltoides* (a temperate species), an increase in the relative contribution of alternate carbon sources was also observed (Funk et al., 2004). However, our current understanding of the responses of isoprene carbon sources to changes in temperature and light levels is poor, and the connection(s) of these responses to changes in leaf primary carbon metabolism (e.g. photosynthesis, photorespiration, and respiration) remains to be determined.

Studies over the last decade have shown or suggested that potential alternate carbon sources include re-fixation of respired CO_2 (Loreto et al., 2004), intermediates from the cytosolic mevalonate (MVA) isoprenoid pathway (Flügge and Gao, 2005; Lichtenthaler, 2010), and intermediates from central carbon metabolism, including pyruvate (Jardine et al., 2010), phosphoenolpyruvate (Rosenstiel et al., 2003), and Glc (Schnitzler et al., 2004). Over 40

years ago, it was also proposed that photorespiratory carbon could directly contribute to isoprene production in plants (Jones and Rasmussen, 1975); however, subsequent studies (Monson and Fall, 1989; Hewitt et al., 1990; Karl et al., 2002) have concluded that photorespiration does not contribute to isoprenoid production.

In this study, we examined the carbon composition of isoprene emitted from tropical tree species under changes in light and temperature, the two key environmental variables that affect isoprene emissions. Using a novel real-time analytical approach, we were able to observe compensatory changes in carbon source contribution to isoprene during thermal ramping at high temperatures, despite the overall isoprene emissions remaining relatively stable. By conducting leaf temperature curves under variable $^{13}\text{CO}_2$ concentrations and applying [2- ^{13}C]Gly leaf labeling, we also reopen the discussion on the role of photorespiration as an alternate source of carbon for isoprenoid formation.

RESULTS

Light Intensity Correlates Positively with Net Photosynthesis and Isoprene Emissions in Mango Leaves

Net photosynthesis measurements were made simultaneously with isoprene emission measurements from mango (*Mangifera indica*) leaves over 0 to 2,000 $\mu\text{mol m}^{-2} \text{s}^{-1}$ PAR at a constant leaf temperature of 30°C. A strong positive correlation between average isoprene emission rates and net photosynthesis rates was observed as these values increased with light intensity ($R^2 = 0.94$; Fig. 1A), with an average of $3.1\% \pm 0.3\%$ of carbon assimilated by net photosynthesis emitted in the form of isoprene over the PAR flux range. This demonstrates the classical tight connection between photosynthesis and isoprene emission under these conditions (Monson and Fall, 1989; Loreto and Sharkey, 1990; Harley et al., 1996). As also observed in these previous studies, at light intensities above 500 $\mu\text{mol m}^{-2} \text{s}^{-1}$ PAR, a decrease in the quantum yields of both net photosynthesis and isoprene emissions occurred as net photosynthesis rates transitioned from light limiting to carboxylation limiting.

Variations in Light Intensity Increase Photosynthetic Carbon Sources for Isoprene in Mango Leaves

To gain additional insight into the connections between net photosynthesis, isoprene emissions, and isoprene carbon sources, PAR curves on mango leaves were conducted under $^{13}\text{CO}_2$. Incorporation of the ^{13}C -label into isoprene was followed through real-time measurements of isoprene isotopologue emission rates with zero to five ^{13}C atoms using proton transfer reaction (PTR)-mass spectrometry (MS) together with gas chromatography (GC)-MS ^{13}C -labeling analysis of isoprene fragment and parent ions C_2 , C_4 , and C_5 . To initiate the experiment, individual mango leaves on plants inside the growth

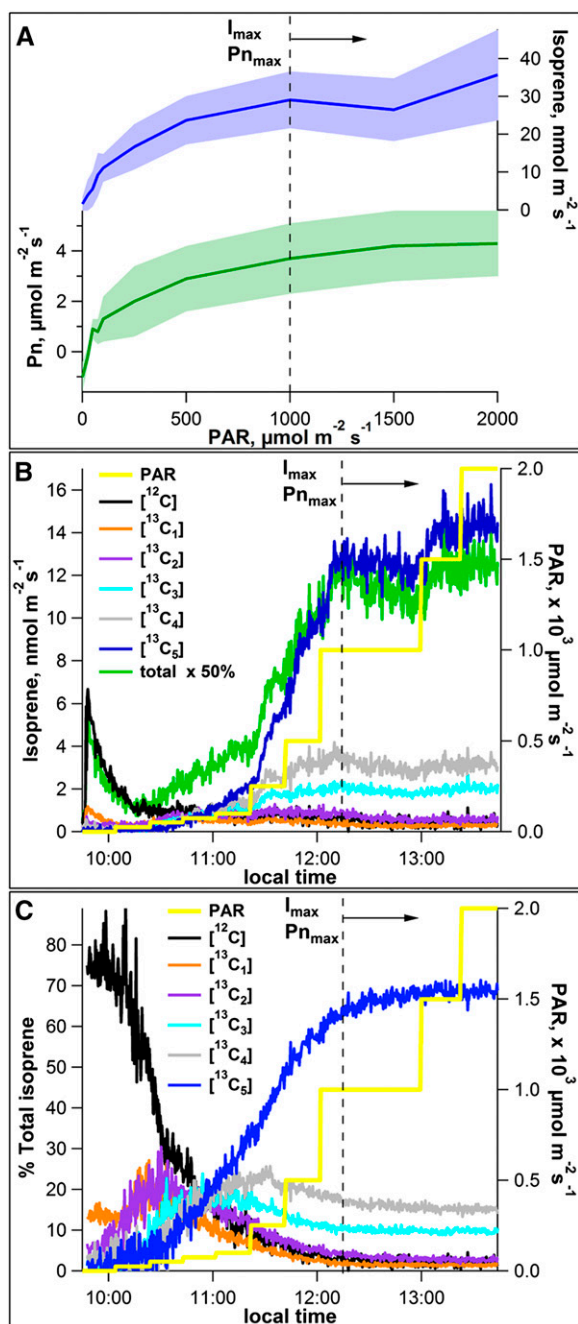


Figure 1. Dependencies of net photosynthesis (Pn) and isoprene emission rates from mango leaves on PAR intensities at a constant leaf temperature (30°C). A, Average of leaf isoprene emissions (GC-MS; blue) and net photosynthesis rates (green) as a function of PAR from four mango leaves. Shaded areas represent ± 1 SD. Also shown are representative PTR-MS time series plots showing the influence of increasing PAR intensity on the dynamics of absolute emissions (B) and relative emissions (percentage of total; C) of [^{12}C]isoprene and [$^{13}\text{C}_{1-5}$]isoprene from a single mango leaf during photosynthesis under $^{13}\text{CO}_2$. Vertical dashed lines represent optimum temperatures for net photosynthesis (Pn_{max}) and isoprene emissions (I_{max}).

chamber were installed in a darkened leaf cuvette exposed to $^{13}\text{CO}_2$. Unlabeled isoprene was released at low levels for 20 to 30 min, the first 15 min of which

was in a darkened cuvette and the remainder of which was at 25 $\mu\text{mol m}^{-2} \text{s}^{-1}$ PAR (representative leaf shown in Fig. 1, B and C). Over the remainder of the experiment, [^{12}C]isoprene emissions remained low, with relative emissions representing less than 5% of total isoprene emissions above 500 $\mu\text{mol m}^{-2} \text{s}^{-1}$ PAR.

During the lowest light intensity (25 $\mu\text{mol m}^{-2} \text{s}^{-1}$ PAR), overall isoprene emissions were low, and significant ^{13}C -labeled isoprene emissions were not detected. However, above the light compensation point for net photosynthesis (20–40 $\mu\text{mol m}^{-2} \text{s}^{-1}$ PAR), emissions of all ^{13}C -labeled isoprene isotopologues were observed. This can also be seen in the GC-MS labeling analysis of isoprene parent and fragment ions (Supplemental Fig. S1). [^{12}C]isoprene was gradually replaced with ^{13}C -labeled isoprene, with [$^{13}\text{C}_5$]isoprene dominating by 76 to 95 min after the experiment started (100 $\mu\text{mol m}^{-2} \text{s}^{-1}$ PAR; dark blue curves in Fig. 1, B and C). Relative emissions of [$^{13}\text{C}_{1-4}$]isoprene sequentially peaked and then declined. Thus, for PAR fluxes of 0 to 500 $\mu\text{mol m}^{-2} \text{s}^{-1}$, the relative abundances of [^{12}C]isoprene and [$^{13}\text{C}_{1-4}$]isoprene represented a significant fraction of total emissions, although ^{13}C -labeling of isoprene is most likely a function of both PAR intensity and time after reillumination (Fig. 1, B and C).

From 500 to 1,000 $\mu\text{mol m}^{-2} \text{s}^{-1}$ PAR, a strong increase in the absolute emissions of [$^{13}\text{C}_5$]isoprene occurred (from 6 to 16 $\text{nmol m}^{-2} \text{s}^{-1}$), while unlabeled and partially labeled [$^{13}\text{C}_{1-4}$]isoprene emissions remained essentially constant. Thus, despite the persistence of [$^{13}\text{C}_{1-4}$]isoprene at high light intensities, the increase in isoprene emissions is entirely due to recently assimilated $^{13}\text{CO}_2$. This results in a strong increase in the relative emissions of [$^{13}\text{C}_5$]isoprene and a decrease in relative emissions of [^{12}C]isoprene and [$^{13}\text{C}_{1-4}$]isoprene (Fig. 1C). Above 1,000 $\mu\text{mol m}^{-2} \text{s}^{-1}$ PAR, emissions of [$^{13}\text{C}_5$]isoprene essentially saturate although small increases in emissions rates occurred up to 2,000 $\mu\text{mol m}^{-2} \text{s}^{-1}$. This resulted in a stabilization of the relative emissions of [$^{13}\text{C}_5$]isoprene up to 72% of total emissions with the remainder comprised of [^{12}C]isoprene (0.1% of total), [$^{13}\text{C}_1$]isoprene (1.5% of total), [$^{13}\text{C}_2$]isoprene (2.3% of total), [$^{13}\text{C}_3$]isoprene (9.0% of total), and [$^{13}\text{C}_4$]isoprene (15.1% of total). Thus, essentially all isoprene emissions at 2,000 $\mu\text{mol m}^{-2} \text{s}^{-1}$ PAR contained at least one ^{13}C atom with a large fraction (72%) completely ^{13}C -labeled ([$^{13}\text{C}_5$]isoprene). Consistent with the PTR-MS measurements of relative [$^{13}\text{C}_5$]isoprene emissions, the GC-MS data revealed that the increase in isoprene emission ratio R_5 ($^{13}\text{C}_5/^{12}\text{C}_5$) is largely driven by increases in [$^{13}\text{C}_5$]isoprene emissions; [^{12}C]isoprene emissions remained very low and variable at all light levels (Supplemental Fig. S1).

Photosynthesis and Isoprene Emissions Show Classical Temperature Responses in Mango Leaves

Net photosynthesis measurements were made simultaneously with isoprene emission measurements from mango leaves under variations in leaf temperature at

constant PAR of $1,000 \mu\text{mol m}^{-2} \text{s}^{-1}$ and $400 \mu\text{L L}^{-1}$ (parts per million by volume [ppmv]) CO_2 . Both net photosynthesis and isoprene emissions increased together as leaf temperature increased from 25.0°C to 32.5°C (Fig. 2A). Net photosynthesis rates peaked at leaf temperatures between 30.0°C and 32.5°C . Further increases in leaf temperature (32.5°C – 42.0°C) resulted in a strong decline in net photosynthesis rates, whereas isoprene emissions continued to increase, peaking between 37.5°C and 40°C . These results are consistent with previous studies that also revealed different temperature optima for net photosynthesis (approximately 30°C) and isoprene emissions (approximately 40°C ; Laothawornkitkul et al., 2009). At temperatures above the optimum for isoprene emission, a decline in emission was observed, followed by an increase again in some leaves (Fig. 2A). When average isoprene emission rates were regressed against those of net photosynthesis rates over the leaf temperature interval of 25.0°C to 32.5°C , a positive correlation was observed ($r^2 = 0.79$), with $8.4\% \pm 3.1\%$ of net photosynthesis being released as isoprene emissions. By contrast, over the leaf temperature interval of 32.5°C to 42.0°C (where isoprene emissions increased but net photosynthesis rates decreased), a negative correlation was observed ($r^2 = 0.71$). When control temperature curve experiments on mango leaves over the same leaf temperature range were conducted, but in the dark, isoprene emissions remained very low. Significant stimulation of isoprene emissions could not be detected, even at the highest leaf temperatures (data not shown).

Increases in Leaf Temperature Drive Compensatory Responses in Isoprene Carbon Sources in Mango

To further investigate isoprene carbon sources in response to temperature changes, leaf temperature curves were made on leaves exposed to $^{13}\text{CO}_2$. Upon placing the mango leaf in the chamber at 25.0°C with $1,000 \mu\text{mol m}^{-2} \text{s}^{-1}$ PAR, the leaf continued to release ^{12}C isoprene for 20 to 30 min (black curves in Fig. 2, B and C). Following this initial release, ^{12}C isoprene emissions represented less than 4% of total emissions up to leaf temperatures of 32.5°C . Within 5 min of the leaf being exposed to $^{13}\text{CO}_2$ in the light, emissions of all ^{13}C -labeled isoprene isotopologues could be detected. Thus, although the leaf continued to release ^{12}C isoprene for 20 to 30 min following exposure to $^{13}\text{CO}_2$, ^{13}C -labeled isoprene could already be detected within 5 min. These observations likely reflect the replacement of the ^{12}C -substrates by ^{13}C -labeled precursors derived from photosynthesis. After 5 min, $^{13}\text{C}_5$ isoprene increased sharply, dominating emissions within 11 min and stabilizing at 44% of the total emissions within 20 min (dark blue curves in Fig. 2, B and C). Increasing the leaf temperature to 27.5°C resulted in enhanced emission rates of $^{13}\text{C}_{3-5}$ isoprene without significant increases in $^{13}\text{C}_{1-2}$ isoprene emissions. This resulted in an increase in $^{13}\text{C}_5$ isoprene relative emissions to values up to 55% of the total. While further increases in leaf temperatures from 27.5°C to 32.5°C resulted in strong increases in $^{13}\text{C}_5$ isoprene emissions, its

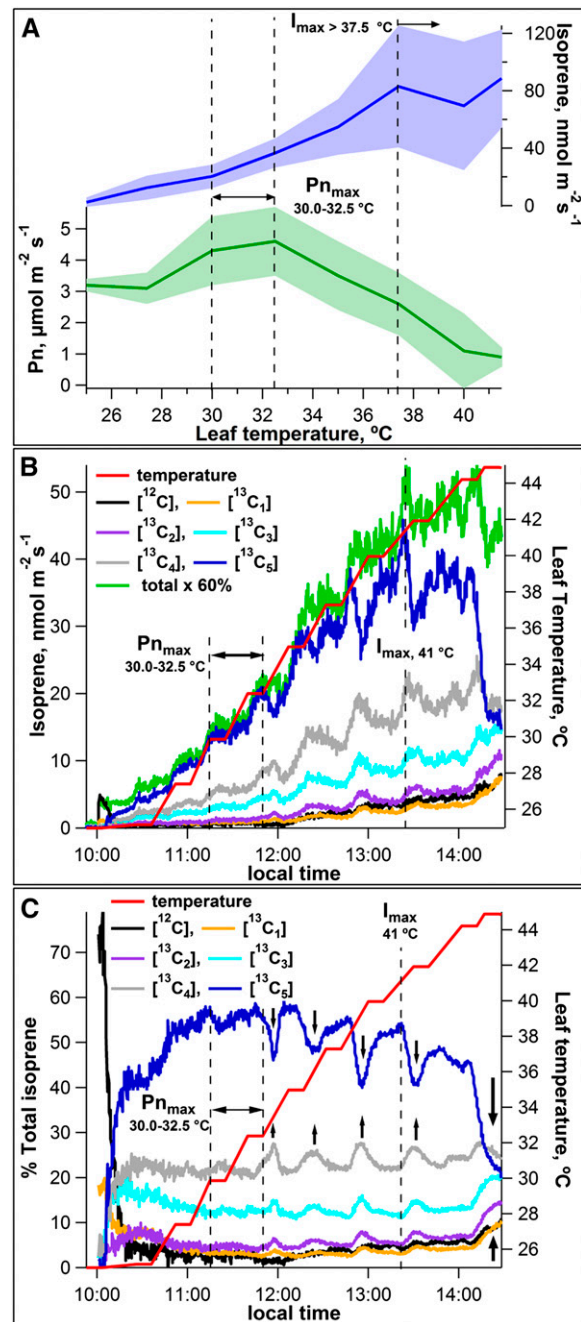


Figure 2. Dependencies of net photosynthesis (Pn) and isoprene emission rates from mango leaves on leaf temperature under constant illumination (PAR of $1,000 \mu\text{mol m}^{-2} \text{s}^{-1}$). A, Average leaf isoprene emissions (GC-MS) and net photosynthesis rates as a function of leaf temperature from four mango leaves. Shaded areas represent ± 1 sd. Also shown are representative PTR-MS time series plots showing the influence of increasing leaf temperature on the dynamics of absolute emissions of ^{12}C isoprene and $^{13}\text{C}_{1-3}$ isoprene (B) and relative isoprene isotopologue emissions rates (percentage of total; C) from a single mango leaf during photosynthesis under $^{13}\text{CO}_2$. Arrows indicate periods of rapid ^{13}C -depletion of isoprenoid intermediates followed by re-enrichment. Vertical dashed lines represent optimum temperature ranges for net photosynthesis (Pn_{max}) and isoprene emissions (I_{max}).

contribution to total emissions only slightly increased, with a maximum value of 59% at 32.5°C.

At leaf temperatures above the optimum for net photosynthesis (30.0°C–32.5°C), an overall trend of declining relative emissions of [$^{13}\text{C}_5$]isoprene with increasing leaf temperature was observed; this decrease was compensated for by increases in relative contributions of [^{12}C]isoprene and [$^{13}\text{C}_{1-3}$]isoprene to maintain high isoprene emissions. At leaf temperatures above 32.5°C, enhanced emission dynamics of all ^{13}C -labeled isoprene isotopologues occurred, including periods of rapid depletion of [$^{13}\text{C}_5$]isoprene followed by partial recovery (most clearly shown in Fig. 2C, vertical arrows).

We also analyzed ^{13}C -labeling patterns of GC-MS fragment and parent ions during the temperature curves under $^{13}\text{CO}_2$. $^{13}\text{C}/^{12}\text{C}$ isoprene emission ratios of C_2 ($^{13}\text{C}_2/^{12}\text{C}_2$, $R_2 = \text{mass-to-charge ratio } [m/z] \text{ } 29/27$) and C_4 ($^{13}\text{C}_4/^{12}\text{C}_4$, $R_4 = m/z \text{ } 57/53$) fragment ions and C_5 ($^{13}\text{C}_5/^{12}\text{C}_5$, $R_5 = m/z \text{ } 73/68$) parent ions were calculated as a function of leaf temperature. Consistent with the PTR-MS studies of relative [$^{13}\text{C}_5$]isoprene emissions, the peak in R_2 , R_4 , and R_5 (Fig. 3A) occurred at the same temperature as the optimum temperature for net photosynthesis (32.5°C; Fig. 3B). Also consistent with the PTR-MS observations of absolute [$^{13}\text{C}_5$]isoprene emissions, GC-MS analysis revealed that the absolute emissions of [$^{13}\text{C}_5$]isoprene peaked at substantially higher temperatures than net photosynthesis (37.5°C–40.0°C), whereas [^{12}C]isoprene emissions remained low up to 32.5°C, followed by an increase with temperature (Fig. 3C).

Temperature and $^{13}\text{CO}_2$ Responses in Shimbillo

To extend the temperature study to a second tropical species and to examine responses under enhanced and suppressed photorespiratory conditions, temperature response curves were conducted on shimbillo (*Inga edulis*)

leaves under different $^{13}\text{CO}_2$ atmospheres (low, 150 ppmv; medium, 300 ppmv; and high, 800 ppmv; Fig. 4). At standard conditions (30°C leaf temperature and 1,000 $\mu\text{mol m}^{-2} \text{s}^{-1}$ PAR), total isoprene emissions were much higher under the medium $^{13}\text{CO}_2$ concentrations (total isoprene emissions, 80 $\text{nmol m}^{-2} \text{s}^{-1}$) than low (total isoprene emissions, 17 $\text{nmol m}^{-2} \text{s}^{-1}$) and high (total isoprene emissions, 35 $\text{nmol m}^{-2} \text{s}^{-1}$) $^{13}\text{CO}_2$ concentrations. These results are consistent with what has been previously reported, where isoprene emissions show a peak around 300 ppmv CO_2 and decline at lower and higher concentrations (Affek and Yakir, 2002). However, this pattern was broken at leaf temperatures above 40°C, where total isoprene emissions under high $^{13}\text{CO}_2$ concentrations were similar to those under medium $^{13}\text{CO}_2$ concentrations.

Similar to the overall response of the mango leaves at 400 ppmv, under the low (150 ppmv) and medium (300 ppmv) $^{13}\text{CO}_2$ concentrations, absolute [$^{13}\text{C}_5$]isoprene emissions were stimulated by leaf temperature increases but then declined at higher leaf temperatures (Fig. 4, A and B). As with the mango leaves, this decline in [$^{13}\text{C}_5$]isoprene emissions was accompanied by an increase in unlabeled and partially labeled isoprene emissions. This resulted in a clear optimum leaf temperature, where the relative [$^{13}\text{C}_5$]isoprene emissions (percentage total) were maximized. Relative to medium $^{13}\text{CO}_2$ concentrations, photorespiratory conditions (low $^{13}\text{CO}_2$) resulted in a reduction in the leaf temperature, at which [$^{13}\text{C}_5$]isoprene emissions peaked (percentage total). Under medium $^{13}\text{CO}_2$ concentrations, [$^{13}\text{C}_5$]isoprene emissions reached at maximum of 78.2% at a leaf temperature of 30.0°C. Under low $^{13}\text{CO}_2$ concentrations, [$^{13}\text{C}_5$]isoprene emissions reached at maximum of 37.6% at a leaf temperature of 27.5°C. In contrast to the low and medium $^{13}\text{CO}_2$ conditions, under the high (800 ppmv) $^{13}\text{CO}_2$ concentrations, absolute [$^{13}\text{C}_5$]isoprene emissions continued to increase up to the highest leaf temperature without a detectable

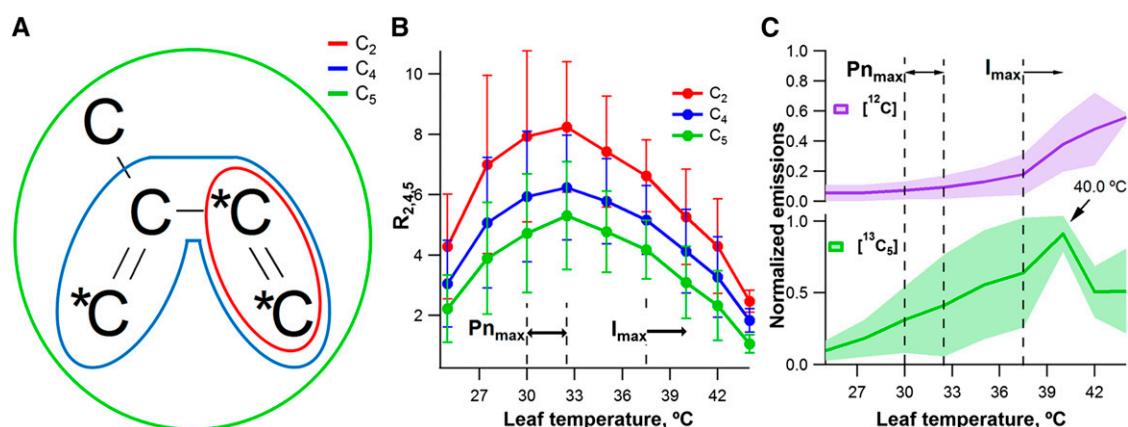


Figure 3. GC-MS ^{13}C -labeling analysis of isoprene emissions from four mango leaves during photosynthesis under $^{13}\text{CO}_2$ as a function of leaf temperature. A, Structure of isoprene GC-MS fragment ions with two carbon atoms (C_2 , red) and four carbon atoms (C_4 , blue) together with the isoprene parent ion with five carbon atoms (C_5 , green). Carbon atoms derived from GA3P and pyruvate are shown as *C and C, respectively. B, Average $^{13}\text{C}/^{12}\text{C}$ isoprene emission ratios of C_2 ($^{13}\text{C}_2/^{12}\text{C}_2$, $R_2 = m/z \text{ } 29/27$) and C_4 ($^{13}\text{C}_4/^{12}\text{C}_4$, $R_4 = m/z \text{ } 57/53$) fragment ions and C_5 ($^{13}\text{C}_5/^{12}\text{C}_5$, $R_5 = m/z \text{ } 73/68$) parent ions. C, Average emission rates for [^{12}C]isoprene ($m/z \text{ } 68$) and [$^{13}\text{C}_5$]isoprene ($m/z \text{ } 73$) normalized to the maximum emissions of [$^{13}\text{C}_5$]isoprene. Vertical dashed lines represent optimum temperature ranges for net photosynthesis (Pn_{max}) and isoprene emissions (I_{max}).

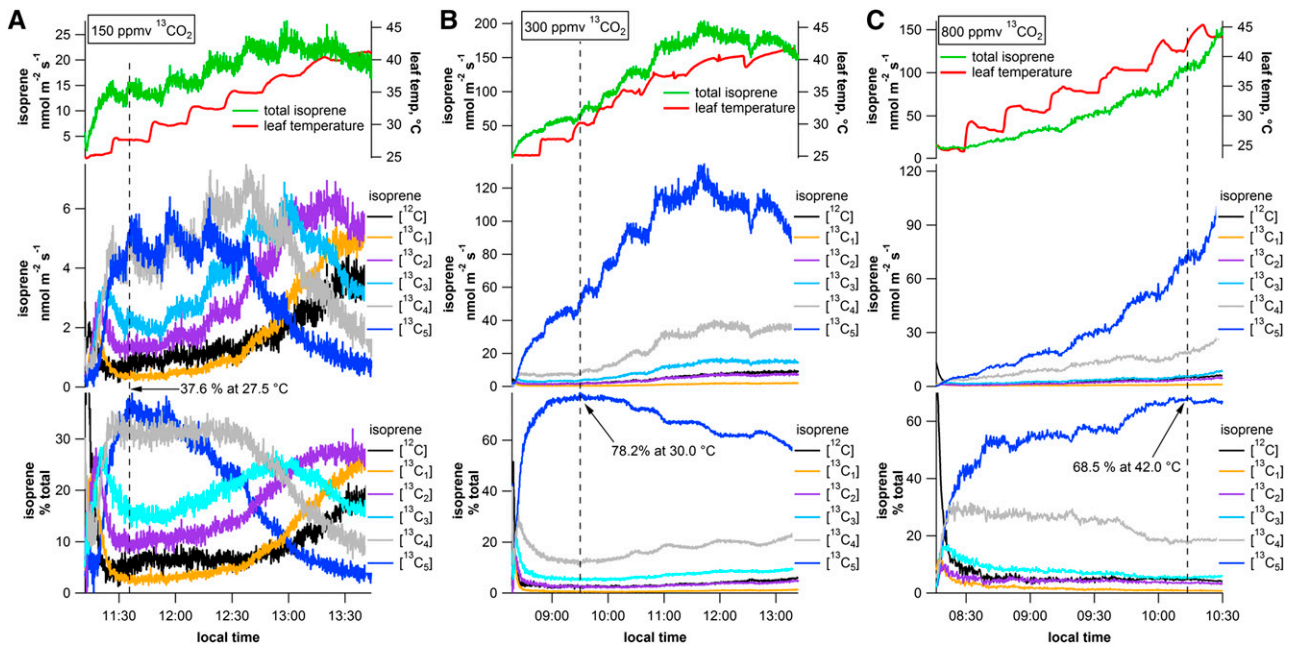


Figure 4. Representative PTR-MS time series plots showing absolute and relative emissions (percentage of total) of ^{12}C isoprene and $^{13}\text{C}_{1-5}$ isoprene as a function leaf temperature from three separate shimbillo leaves exposed to 150 (A), 300 (B), and 800 (C) ppmv $^{13}\text{CO}_2$. Note that increased $^{13}\text{CO}_2$ concentrations strongly enhance the temperature corresponding to the maximum relative emissions of $^{13}\text{C}_5$ isoprene (150 ppmv, 27.5°C; 300 ppmv, 30.0°C; and 800 ppmv, 42.0°C).

decline, paralleling overall isoprene emissions (Fig. 4C). Moreover, photosynthetic conditions under high $^{13}\text{CO}_2$ concentrations resulted in a strong increase in the optimal temperature of $^{13}\text{C}_5$ isoprene emissions (maximum of 68.5% at 42.0°C). Thus, the optimal temperature for relative $^{13}\text{C}_5$ isoprene emissions increased with $^{13}\text{CO}_2$ concentrations (150 ppmv $^{13}\text{CO}_2$, 27.5°C; 300 ppmv $^{13}\text{CO}_2$, 30.0°C; and 800 ppmv $^{13}\text{CO}_2$, 42.0°C).

Gly, a Photorespiratory Intermediate, Is an Alternative Carbon Source for Isoprene

To examine photorespiration as a carbon source for isoprene, labeling studies were conducted with $[2-^{13}\text{C}]\text{Gly}$ fed to detached shimbillo branches through the transpiration stream under constant light and temperature conditions, while simultaneous ^{13}C -labeling analysis of CO_2 (using cavity ring-down spectroscopy [CRDS]) and isoprene (using PTR-MS and GC-MS) was implemented. Emissions of $^{13}\text{CO}_2$ were detected within 5 min of placing the detached stem in $[2-^{13}\text{C}]\text{Gly}$ and reached a maximum roughly 4 h later ($\delta^{13}\text{CO}_2$ of roughly 6,000‰; Fig. 5). Together with the increase in $^{13}\text{CO}_2$ emissions, emissions of $^{13}\text{C}_{1-5}$ isoprene was also stimulated at the expense of ^{12}C isoprene. After 4 h in the $[2-^{13}\text{C}]\text{Gly}$ solution, relative emissions of ^{12}C isoprene declined to 42% of total, while $^{13}\text{C}_{1-5}$ isoprene increased to values 31%, 15%, 5%, 4%, and 3%, respectively. Thus, a large fraction (51%) of isoprene emissions under $[2-^{13}\text{C}]\text{Gly}$ contained one to three ^{13}C atoms. This labeling of isoprene was confirmed by GC-MS measurements (data not

shown). When the stem was placed back in water, emissions of $^{13}\text{CO}_2$ and $^{13}\text{C}_{1-5}$ isoprene quickly decreased to natural abundance levels, while ^{12}C isoprene increased. This result suggests a rapid unlabeled of photorespiratory and isoprene precursor pools and that $[2-^{13}\text{C}]\text{Gly}$ delivered to the leaves via the transpiration stream does not accumulate but is rapidly metabolized.

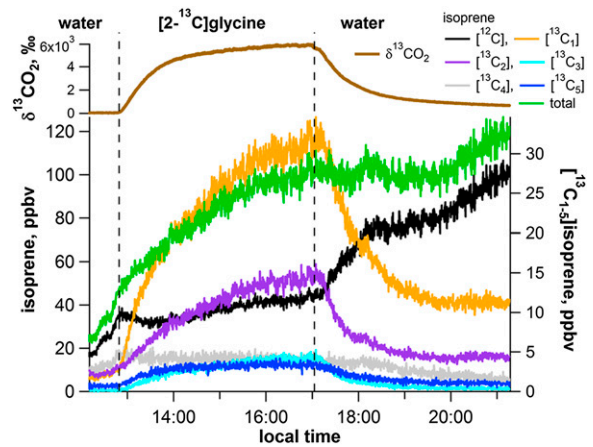


Figure 5. Representative CRDS and PTR-MS time series plot showing ^{13}C -labeling of photorespiratory CO_2 and isoprene during 10 mM $[2-^{13}\text{C}]\text{Gly}$ feeding of a detached shimbillo branch through the transpiration stream under constant light (300–500 $\mu\text{mol m}^{-2} \text{s}^{-1}$ PAR) and air temperature (28°C–30°C). The detached branch was first placed in water and then transferred to the $[2-^{13}\text{C}]\text{Gly}$ solution for 4 h before being replaced in water. ppbv, Parts per billion by volume.

Changes in Gly-Derived Labeling Patterns under Changing Temperature and Photorespiratory Conditions

Leaf temperature curves with [2-¹³C]Gly under photorespiratory conditions (¹²CO₂, 50 and 150 ppmv) were used to evaluate the temperature dependence of putative photorespiratory carbon incorporation into isoprene and CO₂. Under constant light conditions (1,000 μmol m⁻² s⁻¹ PAR), parallel environmental and gas exchange measurements were made as a function of leaf temperature on single detached shimbillo leaves. Isoprene (PTR-MS) and CO₂ (CRDS) ¹³C-labeling dynamics were examined. In leaves exposed to photorespiratory conditions (50 ppmv ¹²CO₂; negative net photosynthesis) and [2-¹³C]Gly, emissions of labeled ¹³CO₂ were observed within minutes of placing the leaf in the solution (Fig. 6A). ¹³CO₂ emissions (0.23–0.26 μmol m⁻² s⁻¹) remained stable for over approximately 1 h, while the leaf temperature was maintained at 30°C and only slightly increased (0.28 μmol m⁻² s⁻¹) when leaf temperatures were elevated to 35°C. A decline in ¹³CO₂ emissions at higher leaf temperatures was observed (>35°C); this may be related to increased stomatal resistance and reduced transpiration rates at the higher leaf temperatures (data not shown). This could increase ¹³CO₂ photoassimilation rates and reduce [2-¹³C]Gly uptake rates, resulting in decreased ¹³CO₂ emissions.

Upon exposure to [2-¹³C]Gly, the label also rapidly appeared as [¹³C₁₋₅]isoprene within minutes, with [¹³C₁]isoprene and [¹³C₂]isoprene being the dominant species. The labeling pattern of isoprene quickly stabilized, with [¹³C₁₋₃]isoprene accounting for 50% to 55% of total isoprene emissions, and remained stable for over 1 h at constant (30°C) leaf temperature. Although emissions of unlabeled [¹²C]isoprene were not strongly stimulated by increases in leaf temperature, those of

[¹³C₁₋₃]isoprene were. In contrast to ¹³CO₂ emissions, which declined at the highest leaf temperatures, [¹³C₁₋₃]isoprene continued to increase up to the highest leaf temperature examined (43.0°C). At 43.0°C, relative emissions were [¹²C]isoprene (27%), [¹³C₁]isoprene (34%), [¹³C₂]isoprene (25%), [¹³C₃]isoprene (10%), and [¹³C₄]isoprene (3%). This contributed to a decrease in [¹²C]isoprene relative emissions with temperature (27% at the highest leaf temperature, 43.0°C). Small emissions of fully ¹³C-labeled [¹³C₅]isoprene emissions could also be detected up to 32.5°C leaf temperature (4%) but returned to background levels at higher leaf temperatures.

The experiment was repeated on leaves under higher, but still photorespiratory, ¹²CO₂ concentrations, (150 ppmv ¹²CO₂). In this case, ¹³CO₂ emissions increased with increasing temperature, up to 37.5°C, where a decline in emissions was observed. Both [¹²C]isoprene and [¹³C₁₋₃]isoprene increased with increasing temperature throughout the experiment; no decrease was observed (Fig. 6B). Relative increases in [¹³C₁₋₃]isoprene were greater than increases in [¹²C]isoprene, resulting in an overall decrease in the relative emissions of [¹²C]isoprene with temperature to a minimum of 43% of total emissions at 37.5°C. At high leaf temperatures, up to 51% of total isoprene emissions had at least one ¹³C ([¹³C₁]isoprene, 31%; [¹³C₂]isoprene, 15%; and [¹³C₃]isoprene, 5%).

DISCUSSION

Coupling of GC-MS, PTR-MS, and CRDS Instruments to a Leaf Photosynthesis System

To finely delineate the contribution of different carbon sources to isoprene under different environmental conditions, we developed a novel analytical approach.

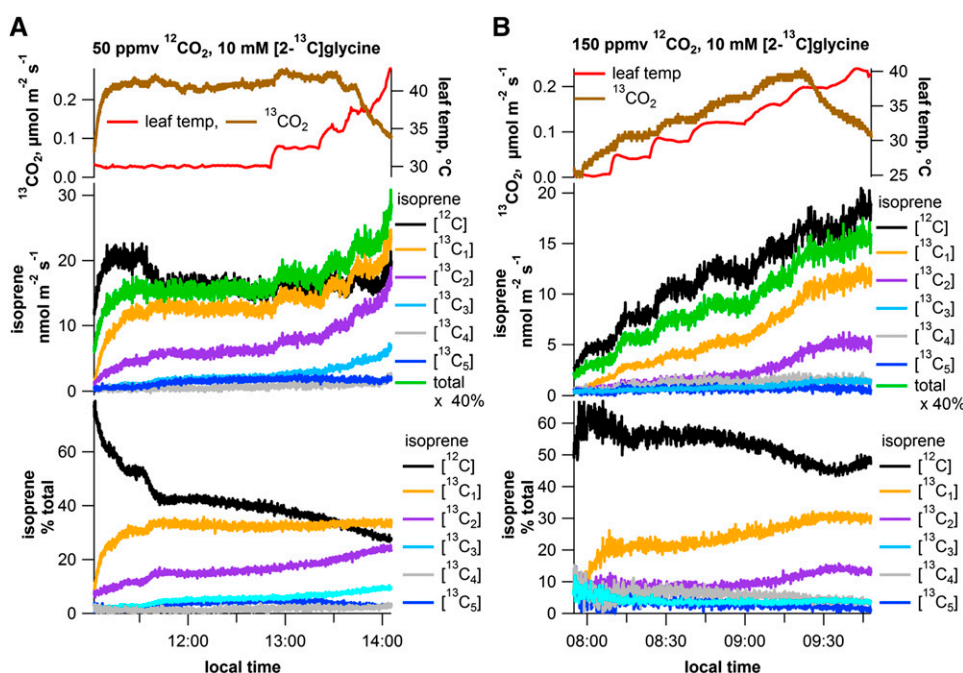


Figure 6. Representative CRDS and PTR-MS time series plots showing the influence of increasing leaf temperature on absolute emissions of photorespiratory ¹³CO₂, [¹²C]isoprene, and [¹³C₁₋₅]isoprene from detached shimbillo leaves in a 10 mM [2-¹³C]Gly solution under 50 ppmv ¹²CO₂ (A) and 150 ppmv ¹²CO₂ (B). Also shown are the relative emissions (percentage of total) of [¹²C]isoprene and [¹³C₁₋₅]isoprene. Note the general pattern of increasing relative emissions of [¹³C₁₋₄]isoprene and a decrease in [¹²C]isoprene with temperature.

The approach is based on the coupling of PTR-MS, thermal desorption (TD) GC-MS, and CRDS instruments to a Li-Cor leaf photosynthesis system. Label was provided through $^{12}\text{CO}_2$ or $^{13}\text{CO}_2$ fumigation or through transpiration stream feeding with a $[2\text{-}^{13}\text{C}]\text{Gly}$ solution. This system enabled us to observe real-time dynamics of $[^{12}\text{C}]\text{isoprene}$ and $[^{13}\text{C}_{1-5}]\text{isoprene}$ leaf emissions during light and temperature curves (PTR-MS) while performing ^{13}C -labeling analysis of isoprene fragment and parent ions C_2 , C_4 , and C_5 (GC-MS). The coupling of both GC-MS and PTR-MS allows us to overcome the limitations of the individual MS systems. PTR-MS only measures signals at a given m/z at unit mass resolution, leaving the results with significant uncertainties around the identity of the responsible compound(s). PTR-MS produces real-time emission data but cannot discriminate between other compounds with the same nominal molecular mass (e.g. isoprene and furan) or determine the difference between a parent ion or an interfering fragment ion from another compound (e.g. isoprene or a fragment of a C_5 green leaf volatile; Fall et al., 2001). High-light and -temperature stresses are known to promote emission of a number of other volatile compounds (Holopainen and Gershenson, 2010), and these compounds could substantially interfere with the PTR-MS signals attributed to isoprene. As the GC-MS provides chromatographic separation of isoprene from other compounds before mass analysis, this data provides an accurate assessment of isoprene carbon sources as a function of light and temperature that can directly be compared with the PTR-MS data. Moreover, because common commercial infrared gas analyzers have very low and unquantified sensitivity to $^{13}\text{CO}_2$, the coupling of the CRDS laser to the photosynthesis system enabled us to measure $^{13}\text{CO}_2$ concentrations during isoprene labeling studies and $^{13}\text{CO}_2$ photorespiratory emission rates during $[2\text{-}^{13}\text{C}]\text{Gly}$ branch and leaf feeding experiments.

Relative Contributions of Different Carbon Sources Do Not Change as a Function of Light Intensity

Following the initiation of $^{13}\text{CO}_2$ labeling during light and temperature curves, mango leaves continued to release $[^{12}\text{C}]\text{isoprene}$ for 20 to 30 min before the $[^{13}\text{C}]$ label began to appear in $[^{13}\text{C}_{1-5}]\text{isoprene}$ (Figs. 1, B and C, and 2, B and C). This release may reflect the time required for the fixed $[^{13}\text{C}]$ to move through metabolism and appear in isoprene, replacing $[^{12}\text{C}]$ in the system. Leaf dimethylallyl pyrophosphate (DMAPP) and/or MEP pathway intermediate pools may be relatively high in mango leaves under our experimental conditions. Using $^{13}\text{CO}_2$ labeling, we found that relative emissions of $[^{13}\text{C}_5]\text{isoprene}$ (percentage of total) determined by PTR-MS, isoprene $^{13}\text{C}/^{12}\text{C}$ isotope ratios (R_2 , R_4 , and R_5) determined by GC-MS for C_2 , C_4 , and C_5 ions, and net photosynthesis rates shared the same optimum in response to leaf temperature and were tightly coupled across all light and temperature conditions studied. Thus, conditions that maximize net photosynthesis rates also

maximize the relative emission rates of $[^{13}\text{C}_5]\text{isoprene}$ (percentage of total). While $[^{13}\text{C}_5]\text{isoprene}$ showed a strong light stimulation in mango leaves, $[^{12}\text{C}]\text{isoprene}$ emissions remained low and were not stimulated by increases in light (Fig. 1; Supplemental Fig. S1). Thus, the increased isoprene emission observed under increasing irradiation (PAR, $>500 \mu\text{mol m}^{-2} \text{s}^{-1}$) is due entirely to synthesis from recently fixed carbon.

Above the Optimum for Net Photosynthesis, the Relative Contribution of Alternate Carbon Sources Increases

Similarly to the situation under increasing illumination in mango leaves, as temperatures increase to the optimum temperature for net photosynthesis, the increase in net photosynthesis rate is driven by increases in the gross photosynthesis rate, and increases in $[^{13}\text{C}_5]\text{isoprene}$ emissions also occur without significant stimulation in $[^{12}\text{C}]\text{isoprene}$ emissions (Figs. 2 and 3). However, at leaf temperatures above the optimum for net photosynthesis, the proportion of carbon derived from alternate carbon sources increased to support high isoprene production rates (Figs. 2 and 3); this is consistent with previous findings in poplar (*Populus* spp.), a temperate tree species (Funk et al., 2004). Consequently, although absolute and relative emissions of $[^{13}\text{C}_5]\text{isoprene}$ were coupled across light curves (Fig. 1; Supplemental Fig. S1), they became decoupled at high leaf temperatures (Figs. 2 and 3): Absolute emissions of $[^{13}\text{C}_5]\text{isoprene}$ peaked at higher leaf temperatures than the optimum for relative $[^{13}\text{C}_5]\text{isoprene}$ emissions. We observed a similar response in a second tropical species, shimbillo, under similar conditions (Fig. 4B), suggesting that the response is typical among isoprene-emitting species.

A Rapid Mechanism for Balancing Availability of Carbon for Isoprene Production under Sharp Temperature Changes

In addition to an overall increase in alternate carbon sources at increased leaf temperatures, a striking short-term compensatory response was observed during sharp temperature ramps in mango at temperatures above the optimum for photosynthesis (Fig. 2, B and C). In these instances, sharp decreases in $[^{13}\text{C}_5]\text{isoprene}$ were mirrored by sharp increases in all partially labeled isoprene species. The increase for each species was proportionate to the relative contribution of each species to total isoprene emission. This response was also observed in shimbillo leaves under similar conditions (Fig. 4B), although it was not quite as pronounced as the mango response. These data suggest that when photosynthesis is unable to provide sufficient substrate to maintain isoprene production during temperature shifts, a rapid mechanism exists to compensate via carbon from alternative sources.

Isoprene synthase (IspS) is responsible for conversion of DMAPP to isoprene (Silver and Fall, 1991). While

DMAPP is found both in the cytosol (from MVA pathway flux) and the chloroplast (from MEP pathway flux), IspS is localized in the chloroplast (Wildermuth and Fall, 1996; Schnitzler et al., 2005; Vickers et al., 2010), so it can only use DMAPP from the chloroplastic pool. Leaf isoprene emission is directly correlated with extractable enzyme activity (Monson et al., 1992) as well as with the amount of IspS in the leaf (Vickers et al., 2010), and IspS levels do not change rapidly in response to changing environmental conditions (Vickers et al., 2011), suggesting that the enzyme itself is not under direct regulation and isoprene production is largely driven by the availability of DMAPP in the chloroplast. Under the assumption that isotopic discrimination by IspS is trivial, we can presume that the decrease in the amount of labeled isoprene observed during temperature ramps is a result of a transient decrease in photosynthetically supplied label and consequently a decrease in photosynthesis-derived MEP pathway flux. The speed of the compensatory response observed in Figure 2 (essentially instantaneous) suggests that an alternative (unlabeled) carbon source is immediately available to the IspS enzyme. This alternative source of carbon may derive from rapid import of glycolysis and/or MVA intermediates (pyruvate/phosphoenolpyruvate and isopentenyl pyrophosphate/DMAPP) from the cytosol and/or from chloroplastic production of unlabeled MEP pathway precursors (pyruvate and glyceraldehyde-3-phosphate). Unlabeled chloroplastic MEP pathway precursors may be generated during photorespiration, starch degradation, and the reassimilation of respiratory and photorespiratory CO₂.

Although it is demonstrated that cross talk exists between the MVA and MEP pathways (Laule et al., 2003), the degree and direction of cross talk is highly variable between species, tissues, developmental stages, etc. Complex and poorly understood regulatory mechanisms exist in plants to ensure that sufficient isoprenoid precursors are available for synthesis of isoprenoid compounds (Rodríguez-Concepción, 2006). It has been shown that prenyl phosphates can be transported across the chloroplast membrane (Flügge and Gao, 2005), and while it is generally thought that cross talk at the prenyl phosphate level occurs at only low levels under normal circumstances, it is clear that exchange of prenyl phosphates between compartments occurs at relatively high levels in a variety of circumstances, in particular, where production of high levels of specific isoprenoids is required (Rodríguez-Concepción, 2006). However, the rate of cross talk has not been accurately quantified.

Investigating Photorespiration as a Source of Alternate Carbon for Isoprene Production

Both recently assimilated and alternate carbon sources are known to contribute to isoprene production in plants, and the relative contribution of different carbon sources changes under changes in environmental conditions, in particular, drought, salt, and heat stress (Loreto

and Delfine, 2000; Funk et al., 2004; Brill et al., 2007) and changes in CO₂/O₂ ratios (Jones and Rasmussen, 1975; Karl et al., 2002; Trowbridge et al., 2012). These former stresses can increase stomatal resistance, resulting in reduced CO₂/O₂ ratios, decreasing rates of net photosynthesis while increasing photorespiratory rates (Wingler et al., 1999; Hoshida et al., 2000). These patterns may be reflected in changes in relative contributions of photosynthetic and alternate carbon sources for isoprene when the flux of immediately fixed carbon is limited (sometimes severely). However, alternate carbon sources for isoprene are relatively poorly defined, and little is known about how they vary during changes in light and temperature, the environmental variables known to have the largest effect on isoprene emissions.

One potential source for the unlabeled isoprene carbon is photorespiration. High temperatures and low CO₂ concentrations are well known to stimulate photorespiration at the expense of photosynthesis, resulting in a decline of net photosynthesis rates (Bauwe et al., 2010; Hagemann et al., 2013). Under increased temperature, the enzyme Rubisco is less able to discriminate between CO₂ and O₂; moreover, the solubility of CO₂ is also reduced, thereby resulting in an increase in the relative concentration of O₂ to CO₂. Consequently, photorespiration increases at increasing temperatures. This makes photorespiration an interesting potential source of alternate carbon under the experimental conditions used here.

It was proposed 40 years ago that photorespiration could serve as an important alternate carbon source for isoprene (Jones and Rasmussen, 1975). In this research study, strong radioactivity was observed in isoprene from leaf slices incubated with [2-¹⁴C]Gly, a photorespiratory intermediate (Fig. 7). The authors noted striking parallels between known controls over isoprene emissions and photorespiration rates, including a stimulation of both processes by temperature and low CO₂ concentrations and suppression by high CO₂ concentrations. Prior to our study, evidence that photorespiratory intermediates could contribute to isoprenoid production in chloroplasts had already been published (Shah and Rogers, 1969). This study demonstrated the appearance of radioactive label in MEP pathway products (including β-carotene during exposure of excised shoots to [2-¹⁴C]glyoxylate and [U-¹⁴C]Ser, both photorespiratory intermediates). However, subsequent studies suggested that there was no close relationship between isoprene emissions and photorespiration (Monson and Fall, 1989; Hewitt et al., 1990; Karl et al., 2002). Most of these studies used reduced oxygen-mixing ratios to inhibit photorespiratory rates; however, this may also interfere with mitochondrial respiration and stimulate fermentation and the accumulation of pyruvate, a substrate for isoprene production (Kimmerer and Macdonald, 1987; Vartapetian et al., 1997; Vartapetian and Jackson, 1997). Thus, low oxygen-mixing ratios may stimulate isoprene production through an increased import of pyruvate into chloroplast (Jardine et al., 2010).

Assuming absolute [¹³C₅]isoprene emission reflects gross photosynthesis rates, while relative emissions

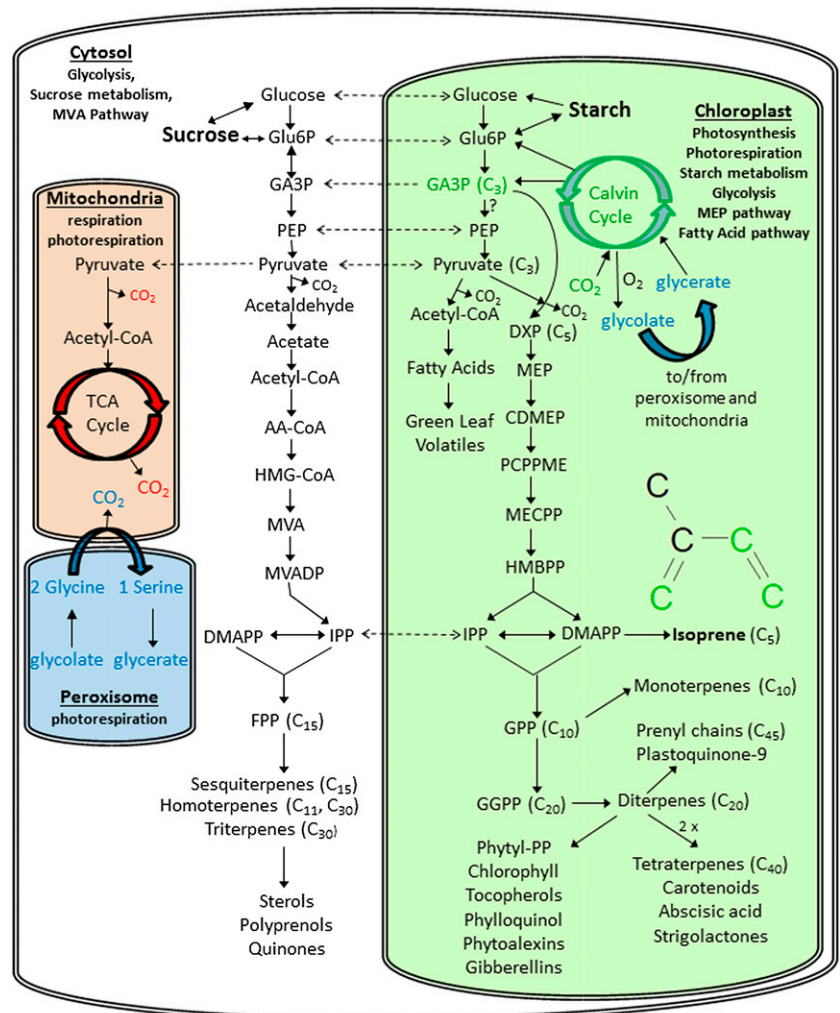
reflect net photosynthesis rates, the observed uncoupling of isoprene emission from net photosynthesis is likely influenced by the high-temperature and/or low-CO₂/O₂ stimulation of respiratory (Loreto et al., 2004) and photorespiratory (Jones and Rasmussen, 1975) CO₂ production. While well known to reduce net photosynthesis rates, these processes may potentially act as alternate carbon sources for isoprene. During ¹³CO₂ labeling, emissions of [¹²C]isoprene and partially labeled [¹³C₁₋₄]isoprene, representing alternate carbon sources, increased with leaf temperature. For example, at leaf temperatures of 45° C, up to 80% of isoprene was emitted as [¹²C]isoprene and [¹³C₁₋₄]isoprene compared with up to 41% at the optimal temperature for net photosynthesis (Fig. 3C). These observations are consistent with previous studies demonstrating increases in alternate carbon contributions for isoprene under conditions known to limit net photosynthesis, including low CO₂ concentrations and drought (Affek and Yakir, 2003; Funk et al., 2004; Trowbridge et al., 2012). In addition to conditions that limit net photosynthesis, those that enhance the rates of alternate carbon sources (e.g. low-CO₂ and high-temperature stimulation of photorespiration) may also

be important contributors to reduced ¹³C-labeling of isoprene under ¹³CO₂.

We decided to examine photorespiration as a potential carbon source more closely using *shimbillo*, a species more amenable to transpiration stream feeding. We first repeated the thermal stress experiments under a range of ¹³CO₂ concentrations (Fig. 4). Under photorespiratory conditions (150 ppmv ¹³CO₂), a reduction in the leaf temperature where emissions of [¹³C₅]isoprene were replaced by partially labeled and unlabeled isoprene was observed (27.5°C under 150 ppmv ¹³CO₂ versus 30°C under 300 ppmv ¹³CO₂). By contrast, under photosynthetic conditions (800 ppmv ¹³CO₂), a dramatic increase in the leaf temperature, where [¹³C₅]isoprene emissions transitioned to unlabeled or partially labeled isoprene emissions, was observed (42.0°C).

Although photorespiratory intermediates can be labeled during photosynthesis under ¹³CO₂, mass spectrometry studies attempting to partition photosynthesis and photorespiration have shown that it is incomplete, likely due to metabolic connections of photorespiratory intermediates with other pathways (Haupt-Herting et al., 2001). Thus, under ¹³CO₂, if photorespiratory carbon

Figure 7. Simplified schematic of isoprenoid metabolism in photosynthetic plant cells and its relationship to photosynthesis, glycolysis, respiration, and photorespiration. Although the MVA pathway is found in the cytosol and the MEP pathway is found in the chloroplast, some cross talk occurs between the pathways through the exchange of intermediates (dashed arrows). CO₂ assimilated by the Calvin cycle, entering the MEP pathway as GA3P and ending up as carbon atoms 1 through 3 of isoprene, is shown in green. Figure modified from Vickers et al., 2009a and 2014. AA-CoA, Acetoacetyl-coenzyme A; CTP, cytidine 5' triphosphate; CDMEP, 4-(cytidine 5'-diphospho)-2-C-methyl-D-erythritol; CMP, cytidine 5' monophosphate; DXP, 1-deoxy-D-xylulose-5-P; FPP, farnesyl pyrophosphate; GPP, geranyl pyrophosphate; GGPP, geranyl geranyl pyrophosphate; G6P, Glc-6-P; HMBPP, 1-hydroxy-2-methyl-2-(E)-butenyl 4-diphosphate; HMG-CoA, (S)-3-hydroxy-3-methylglutaryl-coenzyme A; IPP, isopentenyl pyrophosphate; MECPP, 2-C-methyl-D-erythritol-2,4-cyclodiphosphate; MVAP, mevalonate-5-P; MVADP, mevalonate diphosphate; PEP, phosphoenolpyruvate; PCPPME, 2-phospho-4-(cytidine 5'-diphospho)-2-C-methyl-D-erythritol; Phytlyl-PP, phytlyl pyrophosphate; TCA, tricarboxylic acid.



sources begin to dominate photosynthetic carbon sources for Calvin cycle intermediates, reduced ^{13}C -labeling of isoprene would be expected.

[2- ^{13}C]Gly Labeling Studies Support Photorespiration as an Alternative Carbon Source for Isoprene

Upon feeding of *shimbillo* with [2- ^{13}C]Gly, we observed a rapid incorporation of label into isoprene and CO_2 (Figs. 5 and 6). The results of the *shimbillo* leaf temperature curves under [2- ^{13}C]Gly labeling provide new evidence that both direct (substrate) and indirect (CO_2 reassimilation) photorespiratory carbon processes contribute to isoprene biosynthesis. During photorespiration, the C_1 of Gly is decarboxylated, while the C_2 is used to methylate a second Gly to form Ser via a $^{13}\text{CH}_2$ -tetrahydrofolate intermediate. Thus, the rapid emission of $^{13}\text{CO}_2$ and isoprene with multiple ^{13}C atoms (one to five) demonstrates that the supplied [2- ^{13}C]Gly can undergo several photorespiratory cycles. For example, [2,3- ^{13}C]Ser could form when the supplied [2- ^{13}C]Gly is methylated by $^{13}\text{CH}_2$ -tetrahydrofolate generated from another [2- ^{13}C]Gly. The release of photorespiratory $^{13}\text{CO}_2$ emissions would require the formation of Gly with a ^{13}C atom in the first carbon position ([1- ^{13}C]Gly), which could occur through the entry of photorespiratory intermediates into the Calvin cycle (e.g. glycerate-3-phosphate [GA3P]) followed by the exit of the Gly precursor glycolate into photorespiration. Thus, emissions of $^{13}\text{CO}_2$ from *shimbillo* leaves under [2- ^{13}C]Gly provides evidence of rapid integration of photorespiratory and Calvin cycle intermediates. The output of GA3P from the Calvin cycle with one to three ^{13}C atoms could then explain the ^{13}C -labeling patterns observed in isoprene emissions. However, as $^{13}\text{CO}_2$ emissions were also observed, reassimilation of photorespiratory carbon could also be an important source of ^{13}C in isoprene. When ^{13}C emissions in $^{13}\text{CO}_2$ was quantitatively compared with ^{13}C emissions in [1- ^{13}C]isoprene under [2- ^{13}C]Gly leaf feeding during high leaf temperatures, 10% to 50% of ^{13}C emitted as $^{13}\text{CO}_2$ was emitted as [1- ^{13}C]isoprene. Interpretation of these results, however, is complicated by the reduced transpiration rates and stomatal conductance at high leaf temperatures, leading to a decreased uptake rate of the [2- ^{13}C]Gly solutions and potentially increased reassimilation of $^{13}\text{CO}_2$. Nonetheless, our observations present new evidence that the photorespiratory C_2 cycle and the photosynthetic C_3 Calvin cycle are intimately connected to the MEP pathway for alternate and photosynthetic carbon sources for isoprenoid biosynthesis (Fig. 7).

CONCLUSION

In this study, we show, for the first time, real-time responses of photosynthetic and alternate carbon sources for isoprene synthesis under variations in light and temperature. We also show that one possible alternate carbon

source for isoprene precursors is photorespiration, which is known to become active at the expense of photosynthesis under high temperatures and contribute to the decline in net photosynthesis. While previous research on the effects of CO_2 concentrations on isoprene carbon sources have focused on its potential effects on carbohydrate metabolism (Trowbridge et al., 2012), our results provide new data supporting its role in influencing photorespiratory carbon sources for isoprene. These data support the original suggestion of Jones and Rasmussen (1975) and stand in contrast to studies in the interim that have suggested photorespiration does not provide an alternate carbon source for isoprene.

The processes described here could help maintain the carbon flux through the MEP pathway under high-temperature conditions. This may help maintain the biosynthesis of isoprene (and possibly other isoprenoids including photosynthetic pigments) under stress conditions that reduce photosynthesis rates while increasing photorespiratory rates. Given that the highest isoprene emission rates occur under these conditions, the investment of alternate carbon sources into isoprene biosynthesis is considerable but may be important for helping to protect the photosynthetic machinery from oxidative damage and the activation of stress-related signaling processes (Vickers et al., 2009a, 2014; Karl et al., 2010; Loreto and Schnitzler, 2010; Jardine et al., 2013). By including the representation of photosynthetic and photorespiratory carbon sources of isoprene at high temperatures in mechanistic Earth System models, this study could aid in improving the links between terrestrial carbon metabolism, isoprene emissions, and atmospheric chemistry and improve estimates of the terrestrial carbon budget.

MATERIALS AND METHODS

Isoprene Emissions and Net Photosynthesis

At the Lawrence Berkeley National Laboratory, three growth chambers (E36HO, Percival Scientific) were used to acclimatize nine dwarf mango (*Mangifera indica*) 'Linneaus' (Nam Doc Mai, Top Tropicals) plants for 4 weeks prior to experimentation. This tropical species was selected because of its high reported emissions of isoprene (Jardine et al., 2012, 2013) and the relative ease of obtaining potted plants from a commercial supplier. The plants were maintained under PAR flux density of 300 to 1,500 $\mu\text{mol m}^{-2} \text{s}^{-1}$ (depending on leaf height) with a light period of 7 AM to 5:59 PM, light/dark air temperatures of 30°C/28°C, and ambient CO_2 concentrations of 400 ppmv. The plants were grown in 7.6-L plastic pots (21.6 cm diameter) filled with peat moss soil and watered weekly. Light and temperature curves were carried out on intact individual leaves under $^{12}\text{CO}_2$ and $^{13}\text{CO}_2$ as described below.

Net photosynthesis and isoprene emission rates were quantified from mango leaves using a commercial leaf photosynthesis system (LI-6400XT, Li-Cor) interfaced with a high-sensitivity quadrupole PTR-MS (Ionicon Analytik) and a GC-MS (5975C series, Agilent Technologies). Gas samples were collected on TD tubes and injected into the GC-MS for analysis using an automated TD system (TD100, Markes International) as described below. All tubing and fittings employed downstream of the leaf chamber were constructed with PFA Teflon (Cole Parmer) to prevent isoprene adsorption. Ultra-high-purity hydrocarbon-free air from a zero air generator (737, Pure Air Generator, AADCO Instruments) was humidified with a glass bubbler filled with distilled water and directed to the LI6400XT gas inlet via an overblown tee. At all times, the flow rate of air into the leaf chamber was maintained at 537 mL min^{-1} , the internal fan was set to the maximum speed, and the CO_2

concentration entering the chamber was maintained at 400 ppmv. Using a four-way junction fitting, air exiting the leaf chamber was delivered to the PTR-MS (40 mL min⁻¹) and the TD tube (100 mL min⁻¹ when collecting), with the remainder of the flow diverted to the vent/match valve within the LI6400XT. The excess flow entering the vent/match valve was maintained to at least 200 mL min⁻¹ by loosely tightening the chamber onto the leaf using the tightening nut.

One leaf from each of four mango plants was used to evaluate the response of net photosynthesis and isoprene emissions to changes in PAR and leaf temperature; each curve was generated by averaging the results from the four leaves. Each day of the study for either a PAR or leaf temperature response curve, one leaf near the top of one of the plants was placed in the enclosure, and either leaf temperature or PAR was independently varied while the other variable was held constant. To prevent artificial disturbance to the plants, during gas exchange measurements, the LI6400XT leaf cuvette was placed inside the growth chamber with the plants. Before and after each PAR and leaf temperature curve, background measurements were collected with an empty leaf cuvette. During these background measurements, two TD tube samples were collected with PAR/leaf temperature conditions identical to the first and last values, respectively, in the series. Before and after the introduction of the leaf into the cuvette, continuous isoprene emission rates were acquired using PTR-MS.

For light response curves, measurements were made under constant leaf temperature (30°C) at PAR flux of 0, 25, 50, 75, 100, 250, 500, 1,000, 1,500, and 2,000 $\mu\text{mol m}^{-2} \text{s}^{-1}$. For leaf temperature response curves, measurements were made under constant irradiance (1,000 $\mu\text{mol m}^{-2} \text{s}^{-1}$) at 25°C, 27.5°C, 30°C, 32.5°C, 35°C, 37.5°C, 40°C, and 42°C. In some cases, higher leaf temperatures up to 44°C to 45°C could also be reached. Control experiments were also conducted (two leaves randomly selected from one plant) with the same temperature levels but in the dark (0 $\mu\text{mol m}^{-2} \text{s}^{-1}$) to evaluate the potential for isoprene emissions in the absence of light at elevated temperatures. Following the establishment of a new PAR or leaf temperature level, a delay of 5 min was used prior to data logging to allow the trace gas fluxes to stabilize. After the delay, the reference and sample infrared gas analyzers were matched, leaf environmental and physiological variables were logged, and isoprene emissions were collected on a TD tube (10-min collections for temperature curves and 5-min collections for PAR curves).

¹³C₂ Labeling in Mango

During ¹³C-labeling of isoprene emissions from mango leaves, a cylinder with 99% ¹³CO₂ (Cambridge Scientific) was connected to the LI-6400XT. To maintain a constant approximately 400 ppmv ¹³CO₂ in the reference air entering the leaf cuvette, the CO₂ concentration in the reference chamber was set to 100 ppmv. The difference between ¹³CO₂ concentration as measured by LI-6400XT and the CO₂ concentration set point is due to the reduced sensitivity of the LI-6400XT detector to ¹³CO₂ relative to ¹²CO₂ (roughly 25%). While this configuration allowed for ¹³C-labeling of isoprene, an accurate measurement of net photosynthesis could not be obtained, due to the reduced sensitivity for ¹³CO₂. Therefore, we compared ¹³C-labeling patterns of isoprene as a function of PAR and leaf temperature with isoprene emissions and net photosynthesis under ¹²CO₂. PAR and leaf temperature curves under ¹³CO₂ were conducted using the method described above for ¹²CO₂, and a total of four PAR and four leaf temperature curves were carried out (four different leaves on one plant).

Photorespiratory Carbon Sources Analysis of Isoprene Using ¹³CO₂ and [2-¹³C]Gly Labeling

To evaluate the potential for photorespiratory carbon sources for isoprene, five naturally occurring 5- to 10-m-tall shimbillo (*Inga edulis*) trees growing near the laboratory at the National Institute for Amazon Research were used. This species was selected because detached shimbillo leaves maintained high transpiration rates, and therefore uptake of the [2-¹³C]Gly solutions, for at least 12 h following leaf detachment from the tree. By contrast, mango leaves showed greatly reduced transpiration rates within 1 h following leaf detachment from the tree. Temperature curves (25.0°C, 27.5°C, 30.0°C, 32.5°C, 35.0°C, 37.5°C, 40.0°C, and 42.5°C) were carried out under three different ¹³CO₂ concentrations (150, 300, and 800 ppmv) on attached fully expanded shimbillo leaves (three leaves at each ¹³CO₂ concentration). For [2-¹³C]Gly labeling experiments, the stem of detached shimbillo branchlets (2.7–3.2 g dry weight) were placed in the [2-¹³C]Gly solution, and the leaves were sealed in a 4-L Teflon branch enclosure under constant light (300–500 $\mu\text{mol m}^{-2} \text{s}^{-1}$ PAR) and

air temperature conditions (28°C–30°C) and with 2 L min⁻¹ of hydrocarbon-free air flowing through. Isoprene and CO₂ labeling analysis were performed using PTR-MS, GC-MS, and a cavity ring-down spectrometer for isotopic CO₂ (CRDS model G2201-I, Picarro). Three replicate branchlet labeling experiments were performed on successive days. In addition, temperature curves (30.0°C, 32.5°C, 35.0°C, 37.5°C, 40.0°C, and 42.5°C) were carried out on three detached shimbillo leaves fed with 10 mM [2-¹³C]Gly via the transpiration stream. Detached leaves were placed in tap water before being recut, transported to the laboratory, and placed in the [2-¹³C]Gly solution. The upper portion of the leaf was then immediately placed in the LI-6400XT leaf chamber at 1,000 $\mu\text{mol m}^{-2} \text{s}^{-1}$ PAR and with 537 mL min⁻¹ humidified air flowing through. Two leaves were measured under 50 ppmv ¹²CO₂, and two leaves were measured under 150 ppmv ¹²CO₂ entering the leaf chamber. In addition to leaf physiological variables (e.g. net photosynthesis, transpiration, etc.) measured by the LI-6400XT, [¹²C]isoprene and [¹³C]₂isoprene emissions were measured using PTR-MS in parallel with ¹³CO₂ emissions using CRDS.

TD GC-MS

Isoprene in leaf enclosure air samples was collected by drawing 100 mL min⁻¹ of enclosure air through a TD tube for 5 or 10 min (0.5 and 1.0 L, respectively) by connecting a mass flow controller and a pump downstream of the tube. TD tubes were purchased commercially, filled with Tenax TA, Carbograph 1TD, and Carboxen 1003 adsorbents (Markes International). The TD tube samples were analyzed for isoprene with a TD-100 TD system (Markes International) interfaced to a gas chromatograph/electron impact mass spectrometer with a triple-axis detector (5975C series, Agilent Technologies). After loading a tube in the TD-100 TD system, the collected samples were dried by purging for 4 min with 50 mL min⁻¹ of ultra-high-purity helium (all flow vented out of the split vent) before being transferred (290°C for 5 min with 50 mL min⁻¹ of helium) to the TD-100 cold trap (air toxics) held at 0°C. During GC injection, the trap was heated to 290°C for 3 min while backflushing with carrier gas at a flow of 6.0 mL min⁻¹. Simultaneously, 4 mL min⁻¹ of this flow was directed to the split, and 2 mL min⁻¹ was directed to the column (Agilent DB624, 60 m × 0.32 mm × 1.8 μm). The oven temperature was programmed with an initial hold of 3 min at 40°C followed by an increase to 88°C at 6°C min⁻¹, followed by a hold at 230°C for 10 min. The mass spectrometer was configured for trace analysis with a 15-times detector gain factor and operated in scan mode (*m/z* 35–150). Identification of isoprene from TD tube samples was confirmed by comparison of mass spectra with the U.S. National Institute of Standards and Technology mass spectral library and by comparison of mass spectra and retention time with an authentic liquid standard (10 $\mu\text{g mL}^{-1}$ in methanol, Restek). The GC-MS was calibrated to isoprene by injecting 0.0, 0.5, 1.0, and 2.0 μL of the liquid standard onto separate TD tubes with 100 mL min⁻¹ of ultra-high-purity nitrogen flowing through for 15 min (calibration solution loading rig, Markes International).

The TD GC-MS analysis method for ¹³C-labeled isoprene emissions from mango leaves exposed to ¹³CO₂ was identical to those under ¹²CO₂, except for the parameters of the mass spectrometer. For ¹³CO₂ experiments, the mass spectrometer was also configured for trace analysis with a 15-times detector gain factor but operated in selected ion monitoring mode with 18 different *m/z* values measured sequentially with a 20-ms dwell time each. These include *m/z* 27 to 29 (C₂ isoprene fragment, zero to two ¹³C atoms, respectively), *m/z* 53 to 57 (C₄ isoprene fragment, zero to four ¹³C atoms, respectively), and *m/z* 68 to 73 (C₅ isoprene parent ion, zero to five ¹³C atoms, respectively). ¹³C/¹²C isotope ratios for each sample were calculated for C₂ (¹³C₂H₃/¹²C₂H₃, R₂ = *m/z* 29/27) and C₄ (¹³C₄H₅/¹²C₄H₅, R₄ = *m/z* 57/53) fragment ions as well as C₅ (¹³C₅H₈/¹²C₅H₈, R₅ = *m/z* 73/68) parent ions. It is important to note that R₂, R₄, and R₅ can currently only be considered qualitative indicators of isoprene ¹³C-labeling intensity. This is because just downstream of each GC-MS ¹²C-fragment and parent ion (*m/z* 27, 53, and 68), additional fragments exist, produced, for example, by hydrogen abstractions. ¹³C-labeling of these downstream fragments may increase the signals assumed to be only due to ¹²C-ions (*m/z* 27, 53, and 68). This may result in an underprediction of R₂, R₄, and R₅, which was not accounted for.

PTR-MS

Isoprene emissions were analyzed from the LI6400XT leaf cuvette in real time using a PTR-MS operated with a drift tube voltage of 600 V, temperature of 40°C, and pressure of 200 Pa. The following *m/z* were monitored during each PTR-MS measurement cycle: 21 (H₃¹⁸O⁺) and 32 (O₂⁺) with a dwell time

of 20 ms each and 37 ($\text{H}_2\text{O}-\text{H}_3\text{O}^+$) with a dwell time of 2 ms. Routine maintenance prior to the measurement campaign in California and Manaus, Brazil (ion source cleaning and detector replacement) enabled the system to generate H_3O^+ at high intensity ($1.5\text{--}2.5 \times 10^7$ counts s^{-1} H_3O^+) and purity (O_2^+ and $\text{H}_2\text{O}-\text{H}_3\text{O}^+ < 5\%$ of H_3O^+). During each measurement cycle, the protonated parent ion of [^{12}C]isoprene was measured at m/z 69 with a 2-s dwell time. During ^{13}C -labeling studies, ^{13}C -labeled parent ions of isoprene were also measured with a 2-s dwell time and include m/z 70, [$^{13}\text{C}_1$]isoprene; m/z 71, [$^{13}\text{C}_2$]isoprene; m/z 72, [$^{13}\text{C}_3$]isoprene; m/z 73, [$^{13}\text{C}_4$]isoprene; and m/z 74, [$^{13}\text{C}_5$]isoprene. The PTR-MS was calibrated using 1 ppmv of isoprene gas standard (ozone precursors, Restek) diluted in humidified zero air to six concentrations between 0 and 10.5 nL L^{-1} (ppbv). The PTR-MS sensitivity to [$^{13}\text{C}_{1-5}$]isoprene (m/z 70–74) was assumed to be identical to that measured for [^{12}C]isoprene ($74 \text{ counts s}^{-1} \text{ ppbv}^{-1}$).

Supplementary Data

The following materials are available in the online version of this article.

Supplemental Figure S1. GC-MS ^{13}C -labeling analysis of isoprene emissions from four mango leaves during photosynthesis under $^{13}\text{CO}_2$ as a function of PAR.

ACKNOWLEDGMENTS

We thank Sebastien Biraud, Sara Hefty, Ron Woods, and Rosie Davis at Lawrence Berkeley National Laboratory for advice and support and the Large Biosphere-Atmosphere and Green Ocean Amazon project for logistical support.

Received July 26, 2014; accepted October 11, 2014; published October 15, 2014.

LITERATURE CITED

- Affek HP, Yakir D (2002) Protection by isoprene against singlet oxygen in leaves. *Plant Physiol* **129**: 269–277
- Affek HP, Yakir D (2003) Natural abundance carbon isotope composition of isoprene reflects incomplete coupling between isoprene synthesis and photosynthetic carbon flow. *Plant Physiol* **131**: 1727–1736
- Atkinson R, Arey J (2003) Gas-phase tropospheric chemistry of biogenic volatile organic compounds: a review. *Atmos Environ* **37**: S197–S219
- Bauwe H, Hagemann M, Fernie AR (2010) Photorespiration: players, partners and origin. *Trends Plant Sci* **15**: 330–336
- Brilli F, Barta C, Fortunati A, Lerdau M, Loreto F, Centritto M (2007) Response of isoprene emission and carbon metabolism to drought in white poplar (*Populus alba*) saplings. *New Phytol* **175**: 244–254
- Delwiche CF, Sharkey TD (1993) Rapid appearance of C-13 in biogenic isoprene when (C₂)-C-13 is fed to intact leaves. *Plant Cell Environ* **16**: 587–591
- Fall R, Karl T, Jordon A, Lindinger W (2001) Biogenic C₅ VOCs: release from leaves after freeze-thaw wounding and occurrence in air at a high mountain observatory. *Atmos Environ* **35**: 3905–3916
- Flügge UI, Gao W (2005) Transport of isoprenoid intermediates across chloroplast envelope membranes. *Plant Biol (Stuttg)* **7**: 91–97
- Fortunati A, Barta C, Brilli F, Centritto M, Zimmer I, Schnitzler JP, Loreto F (2008) Isoprene emission is not temperature-dependent during and after severe drought-stress: a physiological and biochemical analysis. *Plant J* **55**: 687–697
- Fuentes J, Wang D, Gu L (1999) Seasonal variations in isoprene emissions from a boreal aspen forest. *J Appl Meteorol* **38**: 855–869
- Funk JL, Mak JE, Lerdau MT (2004) Stress-induced changes in carbon sources for isoprene production in *Populus deltoides*. *Plant Cell Environ* **27**: 747–755
- Goldstein AH, Goulden ML, Munger JW, Wofsy SC, Geron CD (1998) Seasonal course of isoprene emissions from a midlatitude deciduous forest. *J Geophys Res* **103**: 31045–31056
- Guenther A, Karl T, Harley P, Wiedinmyer C, Palmer P, Geron C (2006) Estimates of global terrestrial isoprene emissions using MEGAN (Model of Emissions of Gases and Aerosols from Nature). *Atmos Chem Phys* **6**: 3181–3210
- Hagemann M, Fernie AR, Espie GS, Kern R, Eisenhut M, Reumann S, Bauwe H, Weber APM (2013) Evolution of the biochemistry of the photorespiratory C₂ cycle. *Plant Biol (Stuttg)* **15**: 639–647
- Harley P, Guenther A, Zimmerman P (1996) Effects of light, temperature and canopy position on net photosynthesis and isoprene emission from sweetgum (*Liquidambar styraciflua*) leaves. *Tree Physiol* **16**: 25–32
- Harley P, Vasconcellos P, Vierling L, Pinheiro CCD, Greenberg J, Guenther A, Klinger L, De Almeida SS, Neill D, Baker T, et al (2004) Variation in potential for isoprene emissions among neotropical forest sites. *Glob Change Biol* **10**: 630–650
- Haupt-Herting S, Klug K, Fock HP (2001) A new approach to measure gross CO₂ fluxes in leaves. Gross CO₂ assimilation, photorespiration, and mitochondrial respiration in the light in tomato under drought stress. *Plant Physiol* **126**: 388–396
- Hewitt CN, Monson RK, Fall R (1990) Isoprene emissions from the grass *Arundo donax* L. are not linked to photorespiration. *Plant Sci* **66**: 139–144
- Holopainen JK, Gershenson J (2010) Multiple stress factors and the emission of plant VOCs. *Trends Plant Sci* **15**: 176–184
- Hoshida H, Tanaka Y, Hibino T, Hayashi Y, Tanaka A, Takabe T, Takabe T (2000) Enhanced tolerance to salt stress in transgenic rice that over-expresses chloroplast glutamine synthetase. *Plant Mol Biol* **43**: 103–111
- Jardine K, Abrell L, Jardine A, Huxman T, Saleska S, Arneeth A, Monson R, Karl T, Fares S, Loreto F, et al (2012a) Within-plant isoprene oxidation confirmed by direct emissions of oxidation products methyl vinyl ketone and methacrolein. *Glob Change Biol* **18**: 973–984
- Jardine KJ, Meyers K, Abrell L, Alves EG, Yanez Serrano AM, Kesselmeier J, Karl T, Guenther A, Chambers JQ, Vickers C (2013) Emissions of putative isoprene oxidation products from mango branches under abiotic stress. *J Exp Bot* **64**: 3697–3708
- Jardine KJ, Sommer ED, Saleska SR, Huxman TE, Harley PC, Abrell L (2010) Gas phase measurements of pyruvic acid and its volatile metabolites. *Environ Sci Technol* **44**: 2454–2460
- Jones CA, Rasmussen RA (1975) Production of isoprene by leaf tissue. *Plant Physiol* **55**: 982–987
- Kameel FR, Riboni F, Hoffmann MR, Enami S, Colussi AJ (2014) Fenton oxidation of gaseous isoprene on aqueous surfaces. *J Phys Chem C* (in press)
- Karl T, Fall R, Rosenstiel TN, Prazeller P, Larsen B, Seufert G, Lindinger W (2002a) On-line analysis of the $^{13}\text{CO}_2$ labeling of leaf isoprene suggests multiple subcellular origins of isoprene precursors. *Planta* **215**: 894–905
- Karl T, Harley P, Emmons L, Thornton B, Guenther A, Basu C, Turnipseed A, Jardine K (2010) Efficient atmospheric cleansing of oxidized organic trace gases by vegetation. *Science* **330**: 816–819
- Kesselmeier J, Ciccioli P, Kuhn U, Stefani P, Biesenthal T, Rottenberger S, Wolf A, Vitullo M, Valentini R, Nobre A, et al (2002) Volatile organic compound emissions in relation to plant carbon fixation and the terrestrial carbon budget. *Global Biogeochem Cycles* **16**: 1126–1135
- Kimmerer TW, Macdonald RC (1987) Acetaldehyde and ethanol biosynthesis in leaves of plants. *Plant Physiol* **84**: 1204–1209
- Laothawornkitkul J, Taylor JE, Paul ND, Hewitt CN (2009) Biogenic volatile organic compounds in the Earth system. *New Phytol* **183**: 27–51
- Laule O, Fürholz A, Chang HS, Zhu T, Wang X, Heifetz PB, Gruitsem W, Lange M (2003) Crosstalk between cytosolic and plastidial pathways of isoprenoid biosynthesis in *Arabidopsis thaliana*. *Proc Natl Acad Sci USA* **100**: 6866–6871
- Lerdau M, Keller M (1997) Controls on isoprene emission from trees in a subtropical dry forest. *Plant Cell Environ* **20**: 569–578
- Lichtenthaler HK (2010) The non-mevalonate DOXP/MEP (deoxyxylulose 5-phosphate/methylerythritol 4-phosphate) pathway of chloroplast isoprenoid and pigment biosynthesis. In CA Rebeiz, C Benning, HJ Bohnert, H Daniell, JK Hooper, HK Lichtenthaler, AR Portis, BC Tripathy, eds, *The Chloroplast: Basics and Applications*. Springer Netherlands, Dordrecht, The Netherlands, pp 95–118
- Loreto F, Delfino S (2000) Emission of isoprene from salt-stressed *Eucalyptus globulus* leaves. *Plant Physiol* **123**: 1605–1610
- Loreto F, Mannozi M, Maris C, Nascetti P, Ferranti F, Pasqualini S (2001) Ozone quenching properties of isoprene and its antioxidant role in leaves. *Plant Physiol* **126**: 993–1000
- Loreto F, Pinelli P, Brancaleoni E, Ciccioli P (2004) ^{13}C labeling reveals chloroplastic and extrachloroplastic pools of dimethylallyl pyrophosphate and their contribution to isoprene formation. *Plant Physiol* **135**: 1903–1907
- Loreto F, Schnitzler JP (2010) Abiotic stresses and induced BVOCs. *Trends Plant Sci* **15**: 154–166

- Loreto F, Sharkey TD** (1990) A gas-exchange study of photosynthesis and isoprene emission in *Quercus rubra* L. *Planta* **182**: 523–531
- Loreto F, Velikova V** (2001) Isoprene produced by leaves protects the photosynthetic apparatus against ozone damage, quenches ozone products, and reduces lipid peroxidation of cellular membranes. *Plant Physiol* **127**: 1781–1787
- Magel E, Mayrhofer S, Muller A, Zimmer I, Hampp R, Schnitzler JP** (2006) Photosynthesis and substrate supply for isoprene biosynthesis in poplar leaves. *Atmos Environ* **40**: S138–S151
- Monson RK, Fall R** (1989) Isoprene emission from aspen leaves: influence of environment and relation to photosynthesis and photorespiration. *Plant Physiol* **90**: 267–274
- Monson RK, Jaeger CH, Adams WW, Driggers EM, Silver GM, Fall R** (1992) Relationships among isoprene emission rate, photosynthesis, and isoprene synthase activity as influenced by temperature. *Plant Physiol* **98**: 1175–1180
- Nguyen TB, Roach PJ, Laskin J, Laskin A, Nizkorodov SA** (2011) Effect of humidity on the composition of isoprene photooxidation secondary organic aerosol. *Atmos Chem Phys* **11**: 6931–6944
- Pacifico F, Harrison SP, Jones CD, Sitch S** (2009) Isoprene emissions and climate. *Atmos Environ* **43**: 6121–6135
- Rodríguez-Concepción M** (2006) Early steps in isoprenoid biosynthesis: multilevel regulation of the supply of common precursors in plant cells. *Phytochem Rev* **5**: 1–15
- Rosenstiel TN, Potosnak MJ, Griffin KL, Fall R, Monson RK** (2003) Increased CO₂ uncouples growth from isoprene emission in an agriforest ecosystem. *Nature* **421**: 256–259
- Schnitzler JP, Graus M, Kreuzwieser J, Heizmann U, Rennenberg H, Wisthaler A, Hansel A** (2004) Contribution of different carbon sources to isoprene biosynthesis in poplar leaves. *Plant Physiol* **135**: 152–160
- Schnitzler JP, Zimmer I, Bachl A, Arend M, Fromm J, Fischbach RJ** (2005) Biochemical properties of isoprene synthase in poplar (*Populus × canescens*). *Planta* **222**: 777–786
- Shah SP, Rogers LJ** (1969) Compartmentation of terpenoid biosynthesis in green plants. A proposed route of acetyl-coenzyme A synthesis in maize chloroplasts. *Biochem J* **114**: 395–405
- Sharkey TD, Loreto F** (1993) Water-stress, temperature, and light effects on isoprene emission and photosynthesis of kudzu leaves. *Plant Physiol* **102**: 159
- Sharkey TD, Singsaas EL** (1995) Why plants emit isoprene. *Nature* **374**: 769–769
- Sharkey TD, Yeh S** (2001) Isoprene emission from plants. *Annu Rev Plant Physiol Plant Mol Biol* **52**: 407–436
- Silver GM, Fall R** (1991) Enzymatic synthesis of isoprene from dimethylallyl diphosphate in aspen leaf extracts. *Plant Physiol* **97**: 1588–1591
- Singsaas EL, Lerdau M, Winter K, Sharkey TD** (1997) Isoprene increases thermotolerance of isoprene-emitting species. *Plant Physiol* **115**: 1413–1420
- Trowbridge AM, Asensio D, Eller ASD, Way DA, Wilkinson MJ, Schnitzler JP, Jackson RB, Monson RK** (2012) Contribution of various carbon sources toward isoprene biosynthesis in poplar leaves mediated by altered atmospheric CO₂ concentrations. *PLoS ONE* **7**: e32387
- Vartapetian BB, Jackson MB** (1997) Plant adaptations to anaerobic stress. *Ann Bot (Lond)* **79**: 3–20
- Vartapetian BB, Pulli S, Fagerstedt K** (1997) Plant response and adaptation to anaerobiosis. *Ann Bot (Lond) (Suppl)* **79**: 1
- Velikova V, Sharkey TD, Loreto F** (2012) Stabilization of thylakoid membranes in isoprene-emitting plants reduces formation of reactive oxygen species. *Plant Signal Behav* **7**: 139–141
- Velikova V, Várkonyi Z, Szabó M, Maslenkova L, Nogueis I, Kovács L, Peeva V, Busheva M, Garab G, Sharkey TD, et al** (2011) Increased thermostability of thylakoid membranes in isoprene-emitting leaves probed with three biophysical techniques. *Plant Physiol* **157**: 905–916
- Vickers CE, Bongers M, Liu Q, Delatte T, Bouwmeester H** (2014) Metabolic engineering of volatile isoprenoids in plants and microbes. *Plant Cell Environ* **37**: 1753–1775
- Vickers CE, Gershenzon J, Lerdau MT, Loreto F** (2009a) A unified mechanism of action for volatile isoprenoids in plant abiotic stress. *Nat Chem Biol* **5**: 283–291
- Vickers CE, Possell M, Cojocariu CI, Velikova VB, Laothawornkitkul J, Ryan A, Mullineaux PM, Nicholas Hewitt C** (2009b) Isoprene synthesis protects transgenic tobacco plants from oxidative stress. *Plant Cell Environ* **32**: 520–531
- Vickers CE, Possell M, Laothawornkitkul J, Ryan AC, Hewitt CN, Mullineaux PM** (2011) Isoprene synthesis in plants: lessons from a transgenic tobacco model. *Plant Cell Environ* **34**: 1043–1053
- Vickers CE, Possell M, Nicholas Hewitt C, Mullineaux PM** (2010) Genetic structure and regulation of isoprene synthase in poplar (*Populus* spp.). *Plant Mol Biol* **73**: 547–558
- Wildermuth MC, Fall R** (1996) Light-dependent isoprene emission (characterization of a thylakoid-bound isoprene synthase in *Salix discolor* chloroplasts). *Plant Physiol* **112**: 171–182
- Wingler A, Quick W, Bungard R, Bailey K, Lea P, Leegood R** (1999) The role of photorespiration during drought stress: an analysis utilizing barley mutants with reduced activities of photorespiratory enzymes. *Plant Cell Environ* **22**: 361–373
- Zeidler J, Lichtenthaler F, May H** (1997) Is isoprene emitted by plants synthesized via the novel isopentenyl pyrophosphate pathway? *J Biosci* **52**: 15–23